Subcellular Localization of ALMS1 Supports Involvement of Centrosome and Basal Body Dysfunction in the Pathogenesis of Obesity, Insulin Resistance, and Type 2 Diabetes

Tom Hearn, Cosma Spalluto, Victoria J. Phillips, Glenn L. Renforth, Nane Copin, Neil A. Hanley, and David I. Wilson

Alström syndrome is a rare autosomal recessive disorder caused by mutations in a novel gene of unknown function, *ALMS1*. Central features of Alström syndrome include obesity, insulin resistance, and type 2 diabetes, and therefore investigating *ALMS1* function stands to offer new insights into the pathogenesis of these common conditions. To begin this process, we have analyzed the subcellular localization and tissue distribution of ALMS1 by immunofluorescence. We show that ALMS1 is widely expressed and localizes to centrosomes and to the base of cilia. Fibroblasts with disrupted ALMS1 assemble primary cilia and microtubule cytoskeletons that appear normal, suggesting that the Alström syndrome phenotype results from impaired function rather than abnormal development. Coupled with recent data on the complex phenotype of Bardet-Biedl syndrome, our findings imply an unexpected central role for basal body and centrosome dysfunction in the pathogenesis of obesity, insulin resistance, and type 2 diabetes. Unraveling the molecular mechanisms underlying the Alström syndrome phenotype will be important in the search for new therapeutic targets for these conditions. *Diabetes* 54:1581–1587, 2005

O besity and type 2 diabetes are prevalent health problems that have significant genetic components (1,2). Type 2 diabetes is a heterogeneous condition characterized by varying degrees of insulin resistance and defective β-cell secretion, with obesity being a major predisposing factor. The molecular mechanisms underlying the pathogenesis of these conditions, in particular obesity and insulin resistance, remain poorly understood (1,3). In addition to using genome-wide and candidate gene approaches to identify susceptibility genes, the complexity of obesity and type 2 diabetes may be dissected by the study of single-gene disorders, as illustrated by the insightful progress made from analyses of the different forms of maturity-onset diabetes of the young (4). Alström syndrome is a rare autosomal recessive disorder characterized by early-onset obesity, insulin resistance, and type 2 diabetes, as well as retinal dystrophy, sensorineural hearing loss, cardiomyopathy, and kidney and liver dysfunction (OMIM 203800) (5–7). We and others have recently established that Alström syndrome is caused by mutations in the novel gene *ALMS1* (8,9), encoding a 461-kDa protein of unknown function. ALMS1 contains a novel tandem repeat domain (TRD), a putative leucine zipper, and, near the NH_2 terminus, a polymorphic stretch of 12–20 glutamic acid residues followed by a run of 7 alanine residues (Fig. 1*A*). The COOH terminus of ALMS1 shows similarity to that of a predicted protein from mouse and macaque that is also of unknown function (9); this region of similarity has been termed the ALMS motif (9).

Interestingly, the phenotype of Alström syndrome overlaps with that of Bardet-Biedl syndrome (BBS), which is thought to be caused by centrosome and/or basal body dysfunction (10–14). The centrosome is the major microtubule organizing center of most animal cells and also has roles in regulating cell cycle progression and cell division (15,16). It comprises a pair of centrioles surrounded by a protein matrix termed pericentriolar material. Basal bodies are centriole-derived structures that serve as templates for the assembly of both motile and nonmotile cilia. Whereas motile cilia are restricted to certain cell types, for example columnar epithelial cells in the respiratory tract, almost all vertebrate cells possess a single nonmotile cilium called a primary cilium (17,18). Recent data (19) suggest that primary cilia have sensory functions, and ciliary dysfunction is strongly implicated in several human disorders in addition to BBS, including polycystic kidney disease, laterality defects, and retinal dystrophy (17,20).

To gain insight into the role of ALMS1, we have investigated its subcellular localization and tissue distribution by immunofluorescence. We show that ALMS1 is widely expressed and localizes to centrosomes and the base of cilia. Coupled with recent data on the function of genes associated with BBS, the subcellular localization of ALMS1 implicates centrosome and basal body dysfunction as a critical mechanism in the pathogenesis of obesity, insulin resistance, and type 2 diabetes.

FIG. 1. Characterization of two ALMS1 antibodies. *A*: Schematic representation of human ALMS1 (not to scale) showing locations of synthetic immunogenic peptides Ag[Nter] (NH$_2$ terminus antigen) and Ag[TRD]. *B*: Western blots of Jurkat whole-cell lysate probed with polyclonal antibodies raised to peptides Ag[Nter] and Ag[TRD]. Both antibodies recognize a band consistent with the predicted molecular weight of ALMS1 of 461 kDa (arrows) plus a band at ~350 kDa (*). Antibodies were preincubated with or without the relevant immunogenic peptide (pep) to test specificity. Loading was assessed by reprobing with anti–γ-tubulin (*lower panels*). Ala, alanine; Glu, glutamic acid; LZ, putative leucine zipper.

RESEARCH DESIGN AND METHODS

We generated polyclonal antibodies to ALMS1 by injecting rabbits with the synthetic peptides MEPEDLPWPGELE and HREKPGTFYQQELP, representing amino acids 1–13 and 625–638 of human ALMS1, respectively. Antibodies were affinity-purified using a Sepharose bead column conjugated to the relevant peptide (CovalAb U.K., Cambridge, U.K.). Antibodies (Sigma-Aldrich, Dorset, U.K.) were obtained to α-tubulin, γ-tubulin, acetylated α-tubulin, insulin, and glucagon (all monoclonal raised in mouse) and γ-tubulin (rabbit polyclonal). An MF20 antibody recognizing sarcomeric myosin heavy chains was obtained from the Developmental Studies Hybridoma Bank (Iowa City, IA). Conjugated secondary antibodies (all raised in goat) are as follows: Alexa Fluor 546 and Alexa Fluor 594 anti-mouse (both from Molecular Probes Europe, Leiden, the Netherlands), fluorescein isothiocyanate anti-mouse (Sigma-Aldrich), Texas Red anti-rabbit (Vector Laboratories, Burlingame, CA), and biotinylated anti-rabbit (Vector Laboratories) used in combination with fluorescein isothiocyanate–streptavidin (Sigma-Aldrich) or Texas Red-streptavidin (Vector Laboratories). All antibodies were used at the recommended dilutions.

Immunoblotting. Jurkat whole-cell lysate was obtained from BD Biosciences (San Jose, CA). Electrophoresis was performed using NuPAGE 3–8% Tris-acetate gels (Invitrogen, Paisley, U.K.) and proteins transferred to nitrocellulose membrane using the Invitrogen XCell II blot module according to the manufacturer's instructions. Blots were incubated in PBS, pH 7.4, containing 0.1% Tween 20 and 2% ECL Advance blocking agent (Amersham Biosciences, Little Chalfont, U.K.) at 4°C overnight. Antibody incubations were performed in blocking solution for 1 h at room temperature followed by three 5-min washes in PBS/0.1% Tween 20. ALMS1 antibodies were used at a concentration of 0.1 μg/ml and were preincubated with or without 10-fold excess of the corresponding immunogenic peptide. Detection was performed using horseradish peroxidase–conjugated secondary antibodies and ECL Advance reagents (Amersham Biosciences) according to the manufacturer's instructions. Full-range Rainbow molecular weight markers were obtained from Amersham Biosciences; AKAP450 detected with a monoclonal antibody (BD Biosciences) was used as an additional high molecular weight size standard (molecular weight 450 kDa).

Cell culture. Cells were grown in chambered slides in Dulbecco's modified Eagle medium supplemented with 10% fetal bovine serum and antibiotics at 37°C and 5% CO$_2$ (reagents from PAA Laboratories, Yeovil, U.K.). For microtubule depolymerization experiments, cells were treated with either 10 μg/ml nocodazole (Sigma-Aldrich) or vehicle alone for 1 h at 37°C and immediately processed for immunocytochemistry, as described below. With local ethical committee permission and informed consent, dermal fibroblasts were obtained from skin biopsies from a normal fetus or an individual with Alström syndrome with known genotype: individual F1Ch, as described by Hearn et al. (8).

Immunochemistry. Cells grown in chambered slides were rinsed briefly in PBS and fixed in methanol/acetone/H$_2$O (2:2:1 dilution) for 5 min at room temperature. Human tissues, obtained with local ethical committee permission and informed consent, were fixed in methanol/acetone/H$_2$O (2:2:1 dilution) or 4% paraformaldehyde in PBS overnight at room temperature, embedded in paraffin wax, and sectioned at 5-μm thickness. Adipose tissue slides were obtained from Abcam (Cambridge, U.K.). For antigen retrieval, slides were immersed in boiling sodium citrate solution (0.01 mol/l, pH 6.0) for up to 20 min. Adult tissue sections were treated with trypsin (1 mg/ml; Sigma-Aldrich) for 1 min at room temperature. Immunochemistry was performed as described previously (21), using ALMS1 antibodies at a concentration of 1 μg/ml. Dehydrated slides were mounted in Vectashield (Vector Laboratories) containing either 4,6-diamidino-2-phenylindole or TO-PRO-3 (Molecular Probes Europe) nuclear counterstain. Images were captured with a Zeiss Axioplan fluorescence microscope and Axiovision software (Carl Zeiss, Welwyn Garden City, U.K.) or with a Leica TCS SP2 laser scanning confocal microscope. Controls included peptide blocking as performed for immunoblot analyses, use of preimmune sera, and omission of primary antibody.

Terminal deoxynucleotidyl transferase-mediated dUTP nick-end labeling assay. We fixed cells in 4% paraformaldehyde/2% sucrose in PBS and detected DNA strand breaks by labeling free 3′-OH termini with fluorescein-conjugated dUTP (in situ cell death detection kit; Roche Diagnostics, Lewes, U.K.). For each cell preparation, we calculated the percentage of typical apoptotic cells in 10 randomly selected fields (40× magnification).

Sequence analysis. To investigate the evolutionary conservation of ALMS1, we used TBLASTN to compare the amino acid sequence to genome sequence data from NCBI (National Center for Biotechnology Information; *Mus musculus*, *Gallus gallus*, and *Drosophila melanogaster*), Sanger (*Danio rerio*, *Caenorhabditis elegans*, *Saccharomyces cerevisiae*), JGI (Joint Genome Institute; *Xenopus tropicalis*, *Takifugu rubripes*, *Ciona intestinalis*, and *Chlamydomonas reinhardtii*), TAIR (the Arabidopsis Information Resource; *Arabidopsis thaliana*), and TIGR (the Institute for Genomic Research; *Trypanosoma brucei*). We masked the TRD (amino acids 540-2201) because its unusual amino acid composition (high serine and threonine content and low methionine, cysteine, asparagine, tryptophan, and arginine content, analyzed using Statistical Anaylsis of Protein Sequences [EBI]) yields database hits based on sequence composition rather than residue order. We also excluded the ALMS motif (amino acids 40374-169) because it shares significant sequence similarity with two otherwise unrelated human proteins (data not shown).
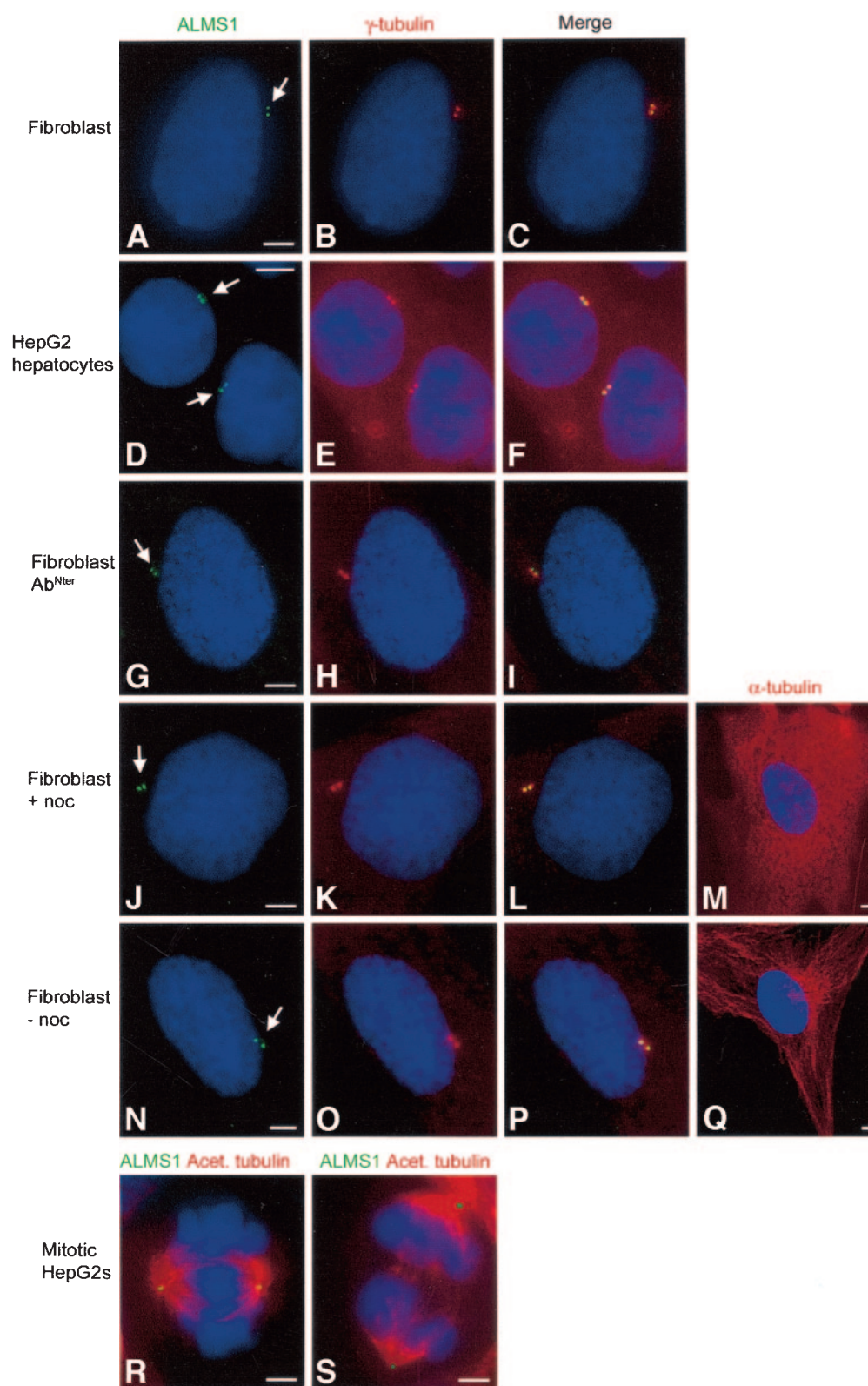
FIG. 2. ALMS1 localizes to the centrosome in cultured human cells. *A–Q*: Immunostaining (green) with anti-ALMS1^TRD (*A*, *D*, *J*, and *N*) and anti-ALMS1^Nter (*G*) is indicated by arrows with the corresponding γ-tubulin (red; *B*, *E*, *H*, *K*, and *O*) and merged (*C*, *F*, *I*, *L*, and *P*) images. Control α-tubulin immunocytochemistry (red) demonstrates microtubule depolymerization according to the presence (*J–M*) or absence (*N–Q*) of nocodazole. *A–C*, *G–Q*: Fetal dermal fibroblasts. *D–F*: HepG2 hepatocytes. *R–S*: Mitotic HepG2 cells immunostained for ALMS1 (green; anti-ALMS1^TRD) and spindle microtubules (red; anti–acetylated α-tubulin). DNA (blue) was visualized with 4,6-diamidino-2-phenylindole in all images. Bars: 4 μm. Ab, antibody; Acet., acetylated; noc, nocodazole.

RESULTS

Generation of two ALMS1 antibodies. We raised polyclonal antibodies to synthetic peptides representing the NH_2 terminus and a section of the TRD of human ALMS1 (Fig. 1*A*). Immunoblot analysis of Jurkat whole-cell lysate showed that both antibodies detect a band consistent with the predicted molecular weight of ALMS1 (461 kDa) plus a band at ~350 kDa (Fig. 1*B*). For both antibodies preincubation with the corresponding immunogenic peptide resulted in loss of both the >450-kDa and ~350-kDa signals (Fig. 1*B*).

ALMS1 localizes to the centrosome in cultured cells. To investigate the subcellular localization of ALMS1, we performed immunocytochemical analyses with anti-ALMS1^TRD. Analysis of the human cell types HepG2
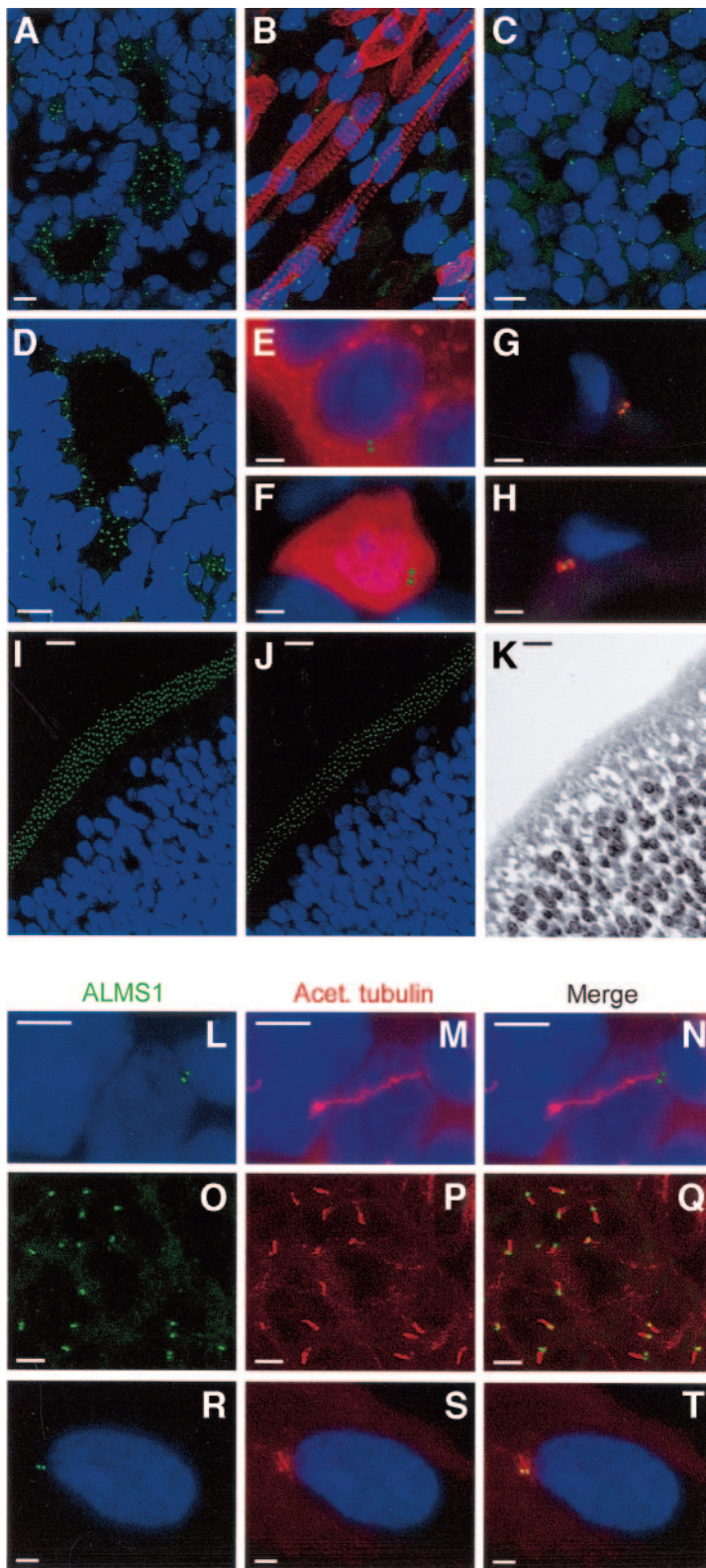
FIG. 3. ALMS1 is widely expressed and localizes to the base of cilia. *A–H*: Immunofluorescent analysis of ALMS1 (green) in fixed human tissues using anti-ALMS1[TRD] (*A–G*) or anti-ALMS1[Nter] (*H*) antibodies, and colabeling (red) with an MF20 antibody recognizing sarcomeric myosin heavy chains (*B*), anti-insulin (*E*), anti-glucagon (*F*), or anti–γ-tubulin (*G* and *H*). Nuclear counterstain (TO-PRO-3 or 4,6-diamidino-2-phenylindole) is in blue. Fetal pancreas (*A*), skeletal muscle (*B*), liver (*C*), kidney (*D*), and brain (consecutive sections) (*I–K*) at 8 weeks postconception, and adult pancreas (*E* and *F*) and adipocytes (*G* and *H*) are shown. *K*: Hematoxylin and eosin staining to demonstrate cellular architecture of corresponding images (*I* and *J*). *L–T*: Fetal kidney tubular cells (*L–N*), nonepithelial fetal kidney cells (*O–Q*), and cultured fetal dermal fibroblasts (*R–T*) immunostained with anti-ALMS1[TRD] (green) and an antibody to visualize cilia raised against acetylated (Acet.) α-tubulin (red). DNA (blue) was visualized with TO-PRO-3 or 4,6-diamidino-2-phenylindole (omitted in *O–Q* for clarity). Bars: 10 μm (*A–D*, *I–K*) or 4 μm (*E–H*, *L–T*).

(hepatocyte), lymphoblastoid, WERI retinoblastoma, and fetal dermal fibroblasts showed that ALMS1 localizes to one or two perinuclear dots per cell (data not shown). This pattern suggested localization to centrosomes, and therefore we performed dual labeling experiments on fetal fibroblasts and on HepG2 cells with anti-ALMS1[TRD] and an antibody to γ-tubulin, a component of the pericentriolar material of centrosomes. We found that ALMS1 is closely

associated with γ-tubulin (Fig. 2*A–F*). Dual labeling of fetal dermal fibroblasts with anti-ALMS1[Nter] (NH₂ terminus ALMS1) and anti–γ-tubulin showed a similar pattern to that observed with anti-ALMS1[TRD] (Fig. 2*G–I*).

To investigate whether localization of ALMS1 to centrosomes is dependent on the intracellular microtubule network, we pretreated fetal fibroblasts and HepG2 cells with nocodazole to depolymerize microtubules. We found that

AS fibroblasts   Control fibroblasts
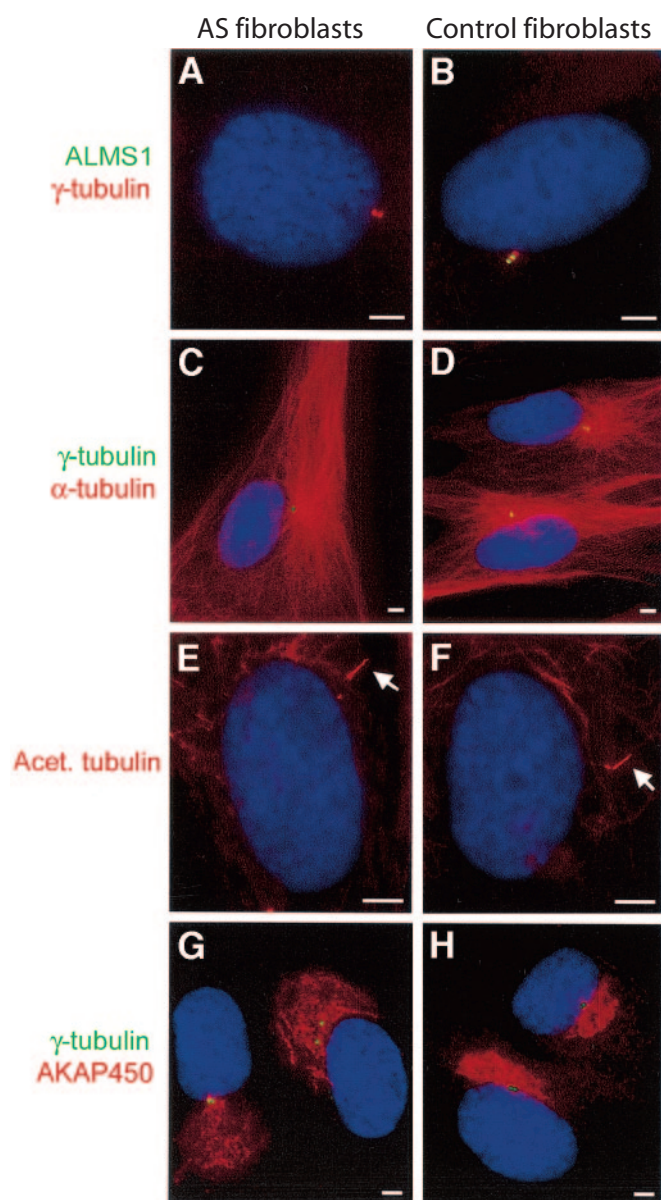
FIG. 4. Immunofluorescent analysis of ALMS1-deficient cultured cells. Dermal fibroblasts derived from an individual with Alström syndrome (AS) were immunostained in parallel with control fetal dermal fibroblasts. *A* and *B*: ALMS1 (green; anti-ALMS1^{TRD}) and the centrosome marker γ-tubulin (red). *C* and *D*: γ-Tubulin (green) and the microtubule marker α-tubulin (red). *E* and *F*: Cilia marker acetylated (Acet.) α-tubulin (red; arrows indicate cilia). *G* and *H*: γ-Tubulin (green) and the Golgi marker AKAP450 (red). DNA (blue) was visualized with 4,6-diamidino-2-phenylindole. Bars: 4 μm.

nocodazole did not affect the association of ALMS1 with the centrosome in either cell type (Fig. 2*J–L* and data not shown). Labeling of mitotic HepG2 cells with anti-ALMS1^{TRD} and an antibody that recognizes spindle microtubules (anti–acetylated α-tubulin) showed that ALMS1 is present at both spindle poles (Fig. 2*R* and *S*).

ALMS1 localizes to centrosomes and the base of cilia. We next investigated the distribution and subcellular localization of ALMS1 in human tissues by immunochemistry. Using anti-ALMS1^{TRD} we detected ALMS1 in all tissues tested, including fetal pancreas, skeletal muscle, liver, kidney, and brain and adult adipose and pancreas (Fig. 3*A–I*). In the latter instance, ALMS1 is expressed in both the α-

and β-cells of the islets, as demonstrated by colabeling with an antibody to glucagon or insulin (Fig. 3*E* and *F*). The labeling pattern in tissues reflected that seen in cultured cells, with one or two perinuclear dots per cell. Notably, in epithelial cells of fetal pancreas, kidney, and brain, signals were located in the apical region (Fig. 3*A*, *D*, and *I*). Anti-ALMS1^{Nter} produced a labeling pattern similar to, though significantly weaker than, that of anti-ALMS1^{TRD} in fixed tissues, for example in fetal brain (Fig. 3*J* and data not shown).

Localization of ALMS1 to the centrosome suggested that ALMS1 may also localize to the centriole-derived structures (basal bodies) at the base of cilia. Consistent with this hypothesis, immunostaining of fetal kidney sections with anti-ALMS1^{TRD} and an antibody to acetylated α-tubulin (a marker for cilia) showed that ALMS1 localizes to the base of primary cilia in both tubular epithelial cells and nonepithelial cells (Fig. 3*L–Q*). ALMS1 also localizes to the base of primary cilia in cultured fibroblasts (Fig. 3*R–T*). The antibody used to mark cilia in these analyses is known to also label centrosomes and a subset of cytoplasmic microtubules (22).

Analysis of ALMS1-deficient fibroblasts. Localization of ALMS1 to the centrosome and base of cilia suggests possible roles for this protein in centrosome/microtubule organization and ciliogenesis, respectively. To investigate these possibilities, we performed immunofluorescent analyses of cultured dermal fibroblasts derived from an individual with Alström syndrome and therefore lacking functional ALMS1 protein: individual F1Ch, as described by Hearn et al. (8). We found that these cells, which are negative for ALMS1 by immunochemistry (Fig. 4*A*), show normal labeling patterns for α-tubulin (microtubules), γ-tubulin (centrosome), and acetylated α-tubulin (primary cilia) (Fig. 4*A–F*). Given the microtubule-dependent association of the Golgi apparatus with the centrosome (23) and the possible role of the centrosome in nucleating the Golgi apparatus (24), we also asked whether Golgi apparatus distribution was abnormal in Alström syndrome cells. Immunostaining for AKAP450/CG-NAP, which localizes to the Golgi apparatus in interphase (25), showed a similar, pericentrosomal distribution in Alström syndrome and control cells (Fig. 4*G* and *H*). Finally, because supression of BBS4 (one of eight proteins known to underlie Bardet-Biedl syndrome) is associated with increased levels of apoptosis in cultured cells (12), we performed terminal deoxynucleotidyl transferase-mediated dUTP nick-end labeling assays on Alström syndrome and control fibroblasts. Apoptosis was not elevated in cells lacking functional ALMS1 (Alström syndrome 1.1%, control 1.3%) (data not shown).

Evolutionary conservation of ALMS1. To investigate the evolutionary conservation of ALMS1, we compared its amino acid sequence to genome sequence databases. We detected similar sequences in the vertebrates *Mus musculus*, *Gallus gallus*, *Xenopus tropicalis*, *Takifugu rubripes*, and *Danio rerio* (*E*-values 0, 1e-27, 2e-12, 1.1e-19, and 7.9e-13, respectively) but not in the invertebrates *Ciona intestinalis*, *Drosophila melanogaster*, *Caenorhabditis elegans*, *Saccharomyces cerevisiae*, *Chlamydomonas reinhardtii*, *Arabidopsis thaliana*, or *Trypanosoma brucei* (*E*-values 0.27, 0.17, 0.13, >10, 1.02, 0.22, and 0.65, respectively).

DISCUSSION

To gain insight into the role of the Alström syndrome protein ALMS1, we have investigated its subcellular localization and tissue distribution by immunofluorescence microscopy. Using antibodies raised to two different regions of the protein, we have shown that ALMS1 is widely expressed and localizes to centrosomes and to the base of cilia. Centrosomal localization is not microtubule dependent, and immunostaining of dividing cells suggests that ALMS1 remains at the centrosome throughout mitosis. In agreement with these findings, ALMS1 has recently been detected in human lymphoblast centrosomes by a mass spectrometry–based proteomic approach (26); localization to the base of cilia has not previously been reported. Notably, immunoblot analysis indicates the existence of a shorter (~350 kDa) isoform in addition to full-length protein (predicted molecular weight 461 kDa). Together with evidence of alternative splicing (8,9), this raises the possibility of further ALMS1 isoforms that await characterization.

The subcellular localization of ALMS1 suggests roles for this protein in microtubule organization, intracellular transport, and the assembly and function of basal bodies and cilia. Intriguingly, there is mounting evidence that BBS, a phenotype with similarities to Alström syndrome, including obesity and retinal dystrophy, is caused by defects in these processes. For example, BBS4 targets cargo to the pericentriolar region (12), BBS proteins are specifically conserved in ciliated organisms including the single-cell organisms *T. brucei* and *C. reinhardtii* (11,27,28), and studies of BBS gene homologues indicate involvement in motor protein–based transport within cilia (29). Immunochemical analysis of ALMS1-deficient fibroblasts showed apparently normal microtubule arrays and primary cilia, suggesting ALMS1 may be important for the function, as opposed to assembly, of these structures. Consistent with this hypothesis, database searches suggest that ALMS1 is restricted to vertebrates and is therefore not required for ciliogenesis in invertebrates. Significantly, BBS4-null mice assemble both motile and nonmotile cilia but lack spermatozoa flagella (11). This finding illustrates different requirements for cilia and flagella assembly in mammals and raises the possibility that reduced fertility in males with Alström syndrome (5) may be caused by a defect in flagella formation.

In summary, this report, together with a proteomic study (26), provides the first clues as to the role of ALMS1 and suggests a functional link with BBS proteins. Expanding on this understanding will be important because the molecular and cellular features underlying Alström syndrome and BBS already suggest new insights into the pathogenesis of obesity, insulin resistance, and type 2 diabetes that ultimately may offer new targets for therapeutic intervention.

REFERENCES

1. McCarthy MI: Progress in defining the molecular basis of type 2 diabetes mellitus through susceptibility-gene identification (Review). *Hum Mol Genet* 13 (Spec. no. 1):R33–R41, 2004
2. Naggert J, Harris T, North M: The genetics of obesity. *Curr Opin Genet Dev* 7:398–404, 1997
3. Saltiel AR, Kahn CR: Insulin signalling and the regulation of glucose and lipid metabolism. *Nature* 414:799–806, 2001
4. Bell GI, Polonsky KS: Diabetes mellitus and genetically programmed defects in beta-cell function. *Nature* 414:788–791, 2001
5. Russell-Eggitt IM, Clayton PT, Coffey R, Kriss A, Taylor DS, Taylor JF: Alstrom syndrome: report of 22 cases and literature review. *Ophthalmology* 105:1274–1280, 1998
6. Marshall JD, Ludman MD, Shea SE, Salisbury SR, Willi SM, LaRoche RG, Nishina PM: Genealogy, natural history, and phenotype of Alstrom syndrome in a large Acadian kindred and three additional families. *Am J Med Genet* 73:150–161, 1997
7. Alstrom CH, Hallgren B, Nilsson LB, Asander H: Retinal degeneration combined with obesity, diabetes mellitus and neurogenous deafness: a specific syndrome (not hitherto described) distinct from the Laurence-Moon-Bardet-Biedl syndrome: a clinical, endocrinological and genetic examination based on a large pedigree. *Acta Psychiatr Neurol Scand* 34:1–35, 1959
8. Hearn T, Renforth GL, Spalluto C, Hanley NA, Piper K, Brickwood S, White C, Connolly V, Taylor JF, Russell-Eggitt I, Bonneau D, Walker M, Wilson DI: Mutation of ALMS1, a large gene with a tandem repeat encoding 47 amino acids, causes Alstrom syndrome. *Nat Genet* 31:79–83, 2002
9. Collin GB, Marshall JD, Ikeda A, So WV, Russell-Eggitt I, Maffei P, Beck S, Boerkoel CF, Sicolo N, Martin M, Nishina PM, Naggert JK: Mutations in ALMS1 cause obesity, type 2 diabetes and neurosensory degeneration in Alstrom syndrome. *Nat Genet* 31:74–78, 2002
10. Ansley SJ, Badano JL, Blacque OE, Hill J, Hoskins BE, Leitch CC, Kim JC, Ross AJ, Eichers ER, Teslovich TM, Mah AK, Johnsen RC, Cavender JC, Lewis RA, Leroux MR, Beales PL, Katsanis N: Basal body dysfunction is a likely cause of pleiotropic Bardet-Biedl syndrome. *Nature* 425:628–633, 2003
11. Mykytyn K, Mullins RF, Andrews M, Chiang AP, Swiderski RE, Yang B, Braun T, Casavant T, Stone EM, Sheffield VC: Bardet-Biedl syndrome type 4 (BBS4)-null mice implicate Bbs4 in flagella formation but not global cilia assembly. *Proc Natl Acad Sci U S A* 101:8664–8669, 2004
12. Kim JC, Badano JL, Sibold S, Esmail MA, Hill J, Hoskins BE, Leitch CC, Venner K, Ansley SJ, Ross AJ, Leroux MR, Katsanis N, Beales PL: The Bardet-Biedl protein BBS4 targets cargo to the pericentriolar region and is required for microtubule anchoring and cell cycle progression. *Nat Genet* 36:462–470, 2004
13. Mykytyn K, Sheffield VC: Establishing a connection between cilia and Bardet-Biedl Syndrome. *Trends Mol Med* 10:106–109, 2004
14. Snell WJ, Pan J, Wang Q: Cilia and flagella revealed: from flagellar assembly in *Chlamydomonas* to human obesity disorders. *Cell* 117:693–697, 2004
15. Rieder CL, Faruki S, Khodjakov A: The centrosome in vertebrates: more than a microtubule-organizing center. *Trends Cell Biol* 11:413–419, 2001
16. Doxsey S: Re-evaluating centrosome function. *Nat Rev Mol Cell Biol* 2:688–698, 2001
17. Ibanez-Tallon I, Heintz N, Omran H: To beat or not to beat: roles of cilia in development and disease. *Hum Mol Genet* 12 (Spec. no. 1):R27–R35, 2003
18. Wheatley DN, Wang AM, Strugnell GE: Expression of primary cilia in mammalian cells. *Cell Biol Int* 20:73–81, 1996
19. Pazour GJ, Witman GB: The vertebrate primary cilium is a sensory organelle. *Curr Opin Cell Biol* 15:105–110, 2003
20. Pazour GJ, Rosenbaum JL: Intraflagellar transport and cilia-dependent diseases. *Trends Cell Biol* 12:551–555, 2002
21. Piper K, Brickwood S, Turnpenny LW, Cameron IT, Ball SG, Wilson DI, Hanley NA: Beta cell differentiation during early human pancreas development. *J Endocrinol* 181:11–23, 2004
22. Piperno G, LeDizet M, Chang XJ: Microtubules containing acetylated alpha-tubulin in mammalian cells in culture. *J Cell Biol* 104:289–302, 1987
23. Rios RM, Bornens M: The Golgi apparatus at the cell centre. *Curr Opin Cell Biol* 15:60–66, 2003
24. Takatsuki A, Nakamura M, Kono Y: Possible implication of Golgi-nucleating function for the centrosome. *Biochem Biophys Res Commun* 291:494–500, 2002
25. Takahashi M, Shibata H, Shimakawa M, Miyamoto M, Mukai H, Ono Y: Characterization of a novel giant scaffolding protein, CG-NAP, that anchors multiple signaling enzymes to centrosome and the golgi apparatus. *J Biol Chem* 274:17267–17274, 1999

26. Andersen JS, Wilkinson CJ, Mayor T, Mortensen P, Nigg EA, Mann M: Proteomic characterization of the human centrosome by protein correlation profiling. *Nature* 426:570–574, 2003

27. Li JB, Gerdes JM, Haycraft CJ, Fan Y, Teslovich TM, May-Simera H, Li H, Blacque OE, Li L, Leitch CC, Lewis RA, Green JS, Parfrey PS, Leroux MR, Davidson WS, Beales PL, Guay-Woodford LM, Yoder BK, Stormo GD, Katsanis N, Dutcher SK: Comparative genomics identifies a flagellar and basal body proteome that includes the BBS5 human disease gene. *Cell* 117:541–552, 2004

28. Avidor-Reiss T, Maer AM, Koundakjian E, Polyanovsky A, Keil T, Subramaniam S, Zuker CS: Decoding cilia function: defining specialized genes required for compartmentalized cilia biogenesis. *Cell* 117:527–539, 2004

29. Blacque OE, Reardon MJ, Li C, McCarthy J, Mahjoub MR, Ansley SJ, Badano JL, Mah AK, Beales PL, Davidson WS, Johnsen RC, Audeh M, Plasterk RH, Baillie DL, Katsanis N, Quarmby LM, Wicks SR, Leroux MR: Loss of *C. elegans* BBS-7 and BBS-8 protein function results in cilia defects and compromised intraflagellar transport. *Genes Dev* 18:1630–1642, 2004